Jour. of the KGS, Vol. 20, No. 7. September 2004, pp. 159~169

Influence of Rainfall-induced Wetting on Unsaturated Weathered Slopes

강우시 국내 불포화 풍화토 사면에서의 습윤영향 분석

Jeong, Sang-Seom[1] 정 상 섬
Kim, Jae-Hong[2] 김 재 홍
Park, Seong-Wan[3] 박 성 완

요 지

얕은사면 파괴는 지표로 침투하는 강우에 의해 주로 발생한다. 이는 지표수의 침투시 모관흡수력의 감소에 의한 포화깊이 증가에 의해 발생한다. 본 연구에서는 국내의 전형적인 화강풍화토를 대상으로 강우시 사면에서의 습윤영향을 분석하였다. 이를 위하여 filter paper와 tensiometer 실험을 수행하여 함수특성곡선을 산정하였으며, 그에 따른 함수특성곡선의 방정식을 추정하였으며, 기존에 사용되고 있는 Green & Ampt의 포화 깊이 추정식과 수치해석결과를 비교 분석하였다. 본 연구 결과, Green & Ampt모델에 의한 이론 해는 포화깊이를 과소 추정하였으며, 포화깊이가 증가함에 따라 사면안전율은 감소하는 것으로 나타났다. 특히 포화깊이가 약 1.2m이상부터 사면안전율은 현저하게 감소하는 것으로 나타났다.

Abstract

Surface failures of slopes in weathered soil are caused by infiltration due to prolonged rainfall. These failures are mainly triggered by the deepening of the wetting band accompanied by a decrease in suction induced by the infiltrating water. This paper reports trends of rainfall-induced wetting band depth in two types of weathered soils that are commonly found in Korea. Both theoretical and numerical analyses are presented based on the soil-water characteristic curve (SWCC) obtained using filter paper as well as tensiometer tests. It is found that the magnitude of wetting front suction plays a key role in the stability of slopes in weathered soils. Theoretical analysis based on modified Green and Ampt model tends to underestimate the wetting band depth for typical Korean weathered soils. It was also deduced that for Korean weathered soils, the factor of safety drops rapidly once the wetting band depth of 1.2 m is reached.

Keywords : Infiltration, Rainfall, Slope stability, Unsaturated soils, Wetting front suction

1. Introduction

Two-thirds of the total land area of the Korean peninsula is occupied by weathered soils that are formed by physical weathering of granite-gneiss of varying thickness ranging from a few meters up to 40 meters. Many slope failures in these weathered soils are triggered by heavy rainfall that usually occurs between

1 Member, Prof., School of Civil & Environmental Engrg., Yonsei Univ., Seoul, Korea (soj9081@yonsei.ac.kr)
2 Member, Ph. D Student, Dept. of Civil Engrg., Univ. of Colorado, USA
3 Member, Full-time Lecturer, Dept. of Civil & Environmental Engrg., Dankook Univ., Seoul, Korea

the months of June and September. These failures are characterized by relatively shallow failure surfaces (typically 2-3 m depth) that develop parallel to the original slope. The groundwater table is usually located at considerable depth below ground surface and there is no evidence that heavy rainfall causes a rise in the water table sufficient to trigger the shallow failures. Instead, the failures may be attributed to the migration of a wetting front pertaining to rainfall infiltration which results in an increase in moisture content, a decrease in soil matric suction and a decrease in shear strength on the potential failure surface (Lumb, 1975; Rahardjo et al., 1995; Ng and Shi, 1998; Fourie et al., 1999).

Many weathered soils in Korea can be classified as SW or SM according to the Unified Soil Classification System (USCS - see Holtz and Kovacs, 1981). These soils consist mainly of completely weathered material with a shallow cover of residual soil (Lee and de Freitas, 1989). Slope failures observed in these soils tend to be shallow with failure plane approximately parallel to the slope surface (Kim et al., 1994). In Korea, the influence of rainfall on the stability of slopes located in weathered soils is usually established using theoretical equations proposed by Pradel and Raad (1993). Kim et al. (1994) have noted that these theoretical equations generally tend to overestimate the factor of safety of such slopes, resulting in slope failures and extensive damage. This paper aims to evaluate the potential shortcomings of these theoretical equations in predicting the rainfall-induced stability of slopes located in weathered soils. Several seepage analyses using a two-dimensional finite element seepage program are conducted to establish the wetting band depth and the wetting front suction for a wider range of initial conditions. For these analyses, the input parameters for soil governing the groundwater flow are derived from soil water characteristic curves (SWCC) obtained using filter paper and tensiometer tests. The results of this parametric study are compared with theoretical results. These results are also incorporated in slope stability analyses conducted using limit equilibrium based slope stability software.

2. Theoretical Equations

Shallow slope failures in weathered soils are triggered when the wetting band reaches a critical depth. Lumb (1962) has proposed an equation to estimate the wetting band depth on the basis of the initial and the final degrees of saturation:

$$h_w = \frac{k_s \cdot t}{n(S_f - S_o)} \tag{1}$$

where h_w is wetting band depth, k_s is the saturated soil permeability, t is the rainfall duration, n is the porosity, and S_o and S_f are the initial and the final degrees of saturation. Eq. (1) has been used to estimate the location of water table for slope stability analysis (Ng and Shi, 1988; Fourie et al., 1999). However, this equation does not take into account the duration and the intensity of rainfall and the magnitude of matric suction present in the soil. Therefore, it is usually not satisfactory to use this equation for problems involving infiltration of rainfall into an unsaturated soil.

Pradel and Raad (1993) have proposed an equation based on the Green and Ampt model (Green and Ampt, 1911) that considers the intensity and the duration of rainfall, the volumetric water content of the soil and the magnitude of wetting front suction:

$$T = \frac{\mu}{k_s}\left[z_w - \psi \cdot \ln\left(\frac{\psi + z_w}{\psi}\right)\right] \tag{2}$$

where T is the rainfall duration, μ is the difference between the saturated and the initial volumetric water content of the soil, k_s is the saturated soil permeability, z_w is the wetting band depth from the surface of the slope, and Ψ is the wetting front suction defined as the negative pore water pressure just before the soil becomes saturated. The magnitude of Ψ depends on the type of soil. For example, Ψ values ranging from 80 cm ($\approx$ 8 kPa) for coarse-textured soils to 140 cm ($\approx$ 14 kPa) for clays have been reported for soils of southern California (Moore, 1939). Maidment (1993) has reported Ψ values from 0.97 to 156.6 cm ($\approx$ 0.1 to 16 kPa) for 11 different

soil textures classified using the United States Department of Agriculture (USDA) method.

The rate of infiltration of rain water v can be defined by Eq. (3) below:

$$v = k_s\left(\frac{\psi + z_w}{z_w}\right) \tag{3}$$

In order for the soil to become saturated due to infiltration, the rainfall intensity (I) must be greater than or equal to the rate of infiltration (v). Also, the rainfall duration (T) must be longer than the minimum rainfall duration (T_{min}) in order to saturate the slope down to a depth z_w. By taking $T = T_{min}$ and $I_{min} = v$ and combining Eq. (2) and Eq. (3), Eq. (4) was obtained by Pradel and Raad (1993):

$$I_{\min} = \frac{\mu}{T_{\min}}\left[z_w - \psi \cdot \ln\left(\frac{\psi + z_w}{\psi}\right)\right]\left(\frac{z_w + \psi}{z_w}\right) \tag{4}$$

where I_{min} is the minimum rainfall intensity and T_{min} is the minimum rainfall duration. Eq. (4) assumes that the slope is an infinite slope, the soil is initially unsaturated, the slope is continuously wetted by rainfall and there is no loss of water due to evaporation or runoff. Eq. (4) can be used to explore the relationship between wetting band depth, wetting front suction and the duration and intensity of rainfall.

3. Soil-Water Characteristic Curves (SWCC)

For the present study, samples of two different weathered soils were collected from a site near the campus of Yonsei University in Seoul, Korea. The grain-size distribution curves of the two soils are shown in Fig. 1. According to the USCS, these two soils can be classified as SW (well-graded sand) and SM (silty sand). The symbols SW and SM will be used hereafter to denote these two weathered soils.

For groundwater flow through an unsaturated soil, the coefficient of permeability is not a constant but a function of soil suction. Therefore, it is necessary to determine the soil-water characteristic curve (SWCC)

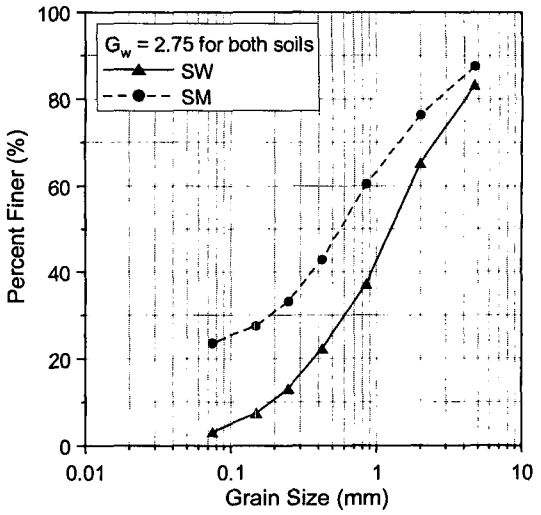

Fig. 1. Grain-size Distribution Curves for the two Weathered Soils

that defines the relationship between the soil suction and volumetric water content (Fredlund and Rahardjo, 1993). SWCC can be used to derive permeability functions for use in unsaturated groundwater flow problems (Fredlund and Rahardjo, 1993). It is also possible to use SWCC to establish saturated shear strength parameters (Vanapalli et al., 1996). For such applications, it is useful to express SWCC by an equation by fitting a curve through experimental data points (Leong and Rahardjo, 1997). In the present study, the SWCC equation was determined based on relationships proposed by van Genuchten (1980) and Fredlund and Xing (1994). These relationships are given by Eq. (5) and Eq. (6), respectively.

$$\Theta = \left[\frac{1}{1 + (\psi/a)^n}\right]^m \tag{5}$$

$$\Theta = \left[\frac{1}{\ln\{e + (\psi/a)^n\}}\right]^m \tag{6}$$

where a, m and n are constants that govern the position and the shape of the SWCC in a Θ-Ψ space, Ψ is the soil suction and Θ is the normalized volumetric water content defined by Eq. (7):

$$\Theta = \frac{\theta_w - \theta_r}{\theta_s - \theta_r} \tag{7}$$

where θ_w is the volumetric water content, θ_r is the

residual volumetric water content and θ_s is the saturated volumetric water content. Parameter a represents scaling factor on suction Ψ, parameter n represents the slope of the SWCC and parameter m represents the residual value of Ψ. By adjusting the values of a, m and n, it is possible to fit a sigmoidal SWCC through experimental data points.

Filter paper test as specified in ASTM D5298-94 (ASTM, 2000) was used for establishing the SWCC for the two weathered soils. Two types of filter papers - Schleicher and Schuell No. 589 and Whatman No.42 - were used. Typical results of filter paper tests are shown in Fig. 2 and Fig. 3. Fig. 2 and Fig. 3 also include the fitted SWCC obtained using Eq. (5) and Eq. (6) that are superimposed on experimental results. The values of constants a, m and n for the fitted SWCC are given in

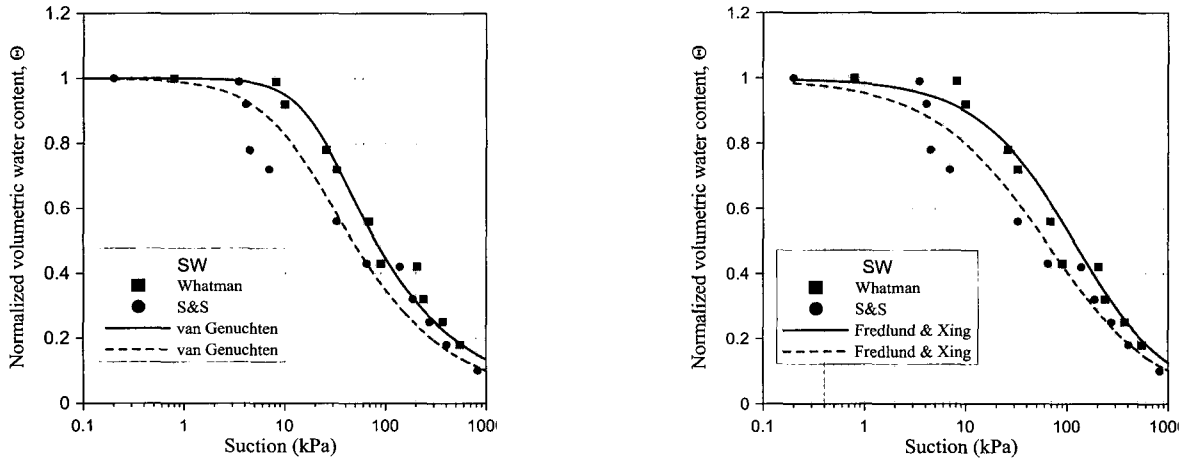

Fig. 2 SWCC for the SW Weathered Soil - Experimental Data and Fitted Curves

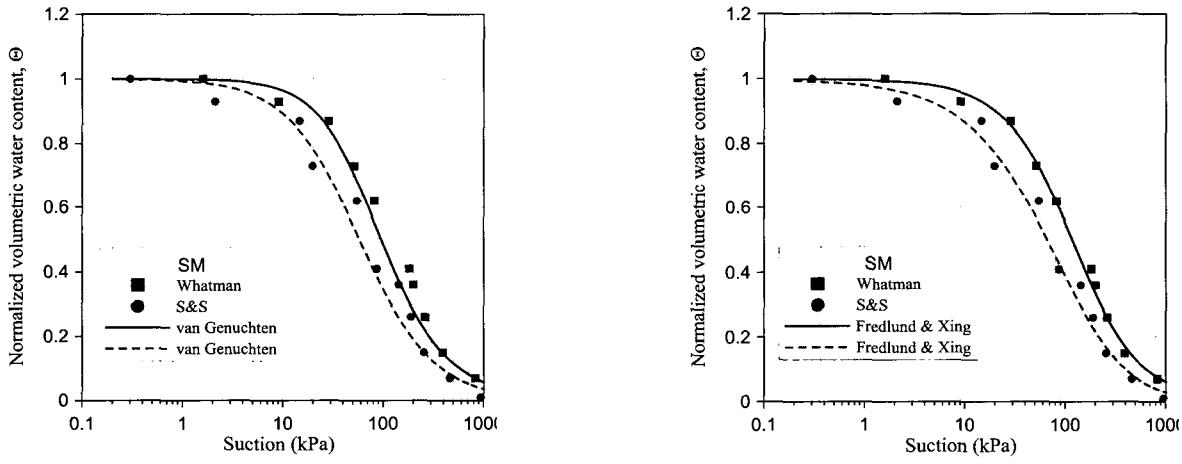

Fig. 3 SWCC for the SM Weathered Soil - Experimental Data and Fitted Curves

Table 1. Curve-fitting Parameters for the SWCC for SW and SM Weathered Soils

Filter paper	Parameter	van Genuchten (1980)		Fredlund & Xing (1994)	
		SW	SM	SW	SM
Whatman No. 42	*a*	22	66	128	136
	n	1.95	1.53	0.86	1.2
	m	0.27	0.69	2.7	2.9
Schleicher & Schuell No. 589	*a*	17	53	78	163
	n	1.25	1.22	0.72	0.9
	m	0.45	0.92	2.9	4.9

Table 1. It was found that tests done using Whatman No. 42 filter paper showed repeatability and gave SWCC that were consistent with SWCC for sandy soils. Leong et al. (2002) reached the same conclusion in their study of factors affecting the filter paper test on residual soils of Singapore.

4. Wetting Front Suction (Ψ)

Wetting front suction Ψ represents the residual value of soil suction just before the soil becomes saturated due to water infiltration. The value of water front suction for a given soil can be obtained experimentally or from empirical relationships (Green and Ampt, 1911; Skaggs and Khaleel, 1982; Rawls et al., 1983; Chow et al., 1988). The magnitude of wetting front suction for a given soil depends primarily on its grain size.

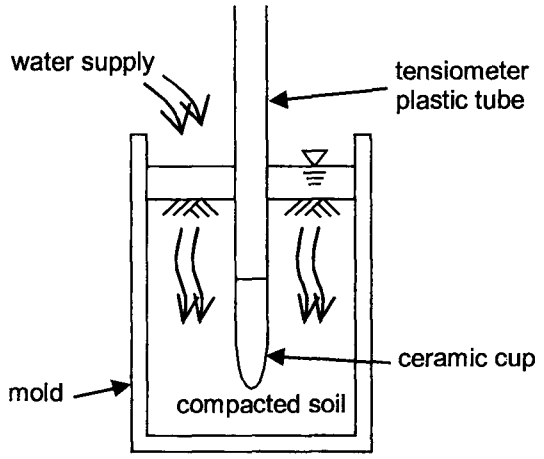

Fig. 4. Schematic diagram of tensiometer test to measure wetting front suction

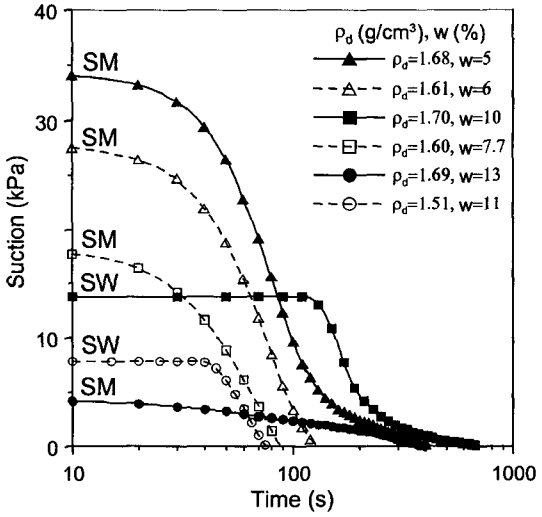

Fig. 5. Variation of Wetting Front Suction with Dry Density and Initial Water Content

In the present study, the values of wetting front suction for the two weathered soils (SW and SM) were obtained in the laboratory using a jet-filled tensiometer. The schematic diagram of the test set-up is shown in Fig. 4. The tensiometer was installed in a 50 cm high mold and weathered soil of known gravimetric moisture content (w, in %) was compacted uniformly around it. The tensiometer was connected to a data logger that recorded its readings at a frequency of 1 Hz (1 reading per second). Water was infiltrated from the top of the compacted soil specimen while monitoring the matric suction at the level of the tensiometer continuously. Several tests at different dry density (ρ_d, in g/cm^3) and w values were conducted. The results for both SW and SM soils are shown in Fig. 5. The initial matric suction value at the tensiometer level depended mainly on the initial w value. For the SW weathered soil, it was not possible to maintain an initial matric suction of more than 8 kPa. The curves for higher dry density samples ($\rho_d \geq 1.68$ g/cm^3) all converge to a wetting front suction of around 2 kPa. However, the curves for samples with $\rho_d < 1.68$ g/cm^3 showed no such convergence and therefore, wetting front suction for these samples could not be measured.

5. Transient Finite Element Seepage Analysis

A two-dimensional finite element program SEEP/W (Geo-Slope, 1998) was used for transient seepage analysis of water infiltration during rainfall. Fig. 6 shows a typical finite element mesh used in the transient seepage analysis. It represents an infinite slope inclined at 45° with respect to horizontal. The slope consists of 12 m deep weathered soil overlying impermeable bedrock that also slopes at 45° with respect to horizontal. The groundwater table is located at the bedrock-weathered soil interface and is considered parallel to the slope. Infinite elements are used at vertical boundaries of the mesh to simulate infinite slope conditions. The top boundary is subjected to a rainfall intensity that is equal to the saturated

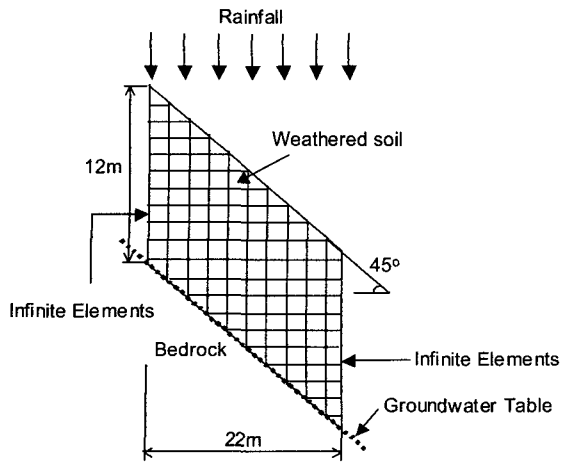

Fig. 6. Finite Element Mesh and Boundary Conditions for Transient Seepage Analysis

permeability of the weathered soil to ensure downward infiltration into the weathered soil layer. The SWCC fitted to the Whatman No. 42 filter paper test results using Eq. (6) (Fredlund and Xing, 1994) is used to derive permeability function for the weathered soil. Table 2 gives the lists of relevant SEEP/W input parameters for both the SW and the SM weathered soils. These input parameters are also used for theoretical calculation of wetting band depth using Eq. (2) (Pradel and Raad, 1993).

The total duration of rainfall is 100 hours. It was divided into 11 time stages - 0.1, 0.5, 1, 2, 3, 5, 10, 24, 48, 72 and 96 hours - and wetting front depth was obtained for each of these 11 time stages. For simplicity, the intensity of rainfall was kept constant for the entire duration of rainfall. For theoretical calculation of wetting band depth, each of these 11 stages was taken as the value of T in Eq. (2) along with constant values of k_s and μ given in Table 2. For a given value of wetting front suction Ψ, such as 20, 40, 60 80, 100 and 120 cm, the wetting band depth z_w can now be calculated using Eq. (2). Similarly, the wetting band depth from a transient seepage analysis is calculated as the normal distance from the surface of the slope at which a contour of -0.2 m pressure head is located. The contour for -0.2 m pressure head is chosen based on the observation from slope stability analyses (described later) that normal distance between the critical failure plane and the surface of the slope was always equal to the normal distance between this contour and the surface of the slope.

6. Wetting Band Depth - Comparison between Theoretical and Numerical Analysis

Fig. 7 and Fig. 8 show the comparison between wetting band depths calculated using Eq. (2) and those obtained from transient seepage analysis. Both theoretical and numerical z_w values increase with increasing rainfall duration. There is good agreement between theoretical and numerical z_w values at Ψ = 80 cm. However, for Ψ < 80 cm, Eq. (2) gives lower z_w values as compared with those given by the numerical analysis. For Ψ > 80 cm, Eq. (2) gives higher z_w values as compared with those given by the numerical analysis. The difference between theoretical and numerical z_w values decreases as Ψ is increased beyond 80 cm. Eq. (2) also appears to be less sensitive to changes in Ψ as compared with the numerical analysis. For example, for SM weathered soil at T = 10 hours, theoretical z_w value changes by less than 10 cm when Ψ is increased from 40 to 120 cm. The corresponding change in numerical z_w value is more than 35 cm. Moreover, the theoretical and numerical analyses show opposite trends when Ψ is plotted against z_w for a given value of T as shown in Fig. 9. Eq. (2) shows an increase in z_w with Ψ whereas numerical analysis shows a decrease in z_w with Ψ. The two trend lines appear to cross each other at a Ψ value close to 80 cm. The overall discrepancy between z_w values obtained from

Table 2. Material Properties for the SW and SM Weathered Soils

Soil Type	k_s (m/s)	θ_i (%)	θ_s (%)	S (%)	S_r (%)	ϕ^b (°)		
						loose	medium	dense
SW	7.08×10^{-7}	23.2	43.1	52	18	10.9	12.9	15.1
SM	1.30×10^{-7}	18.5	43.5	39	19	6.6	7.8	9.1

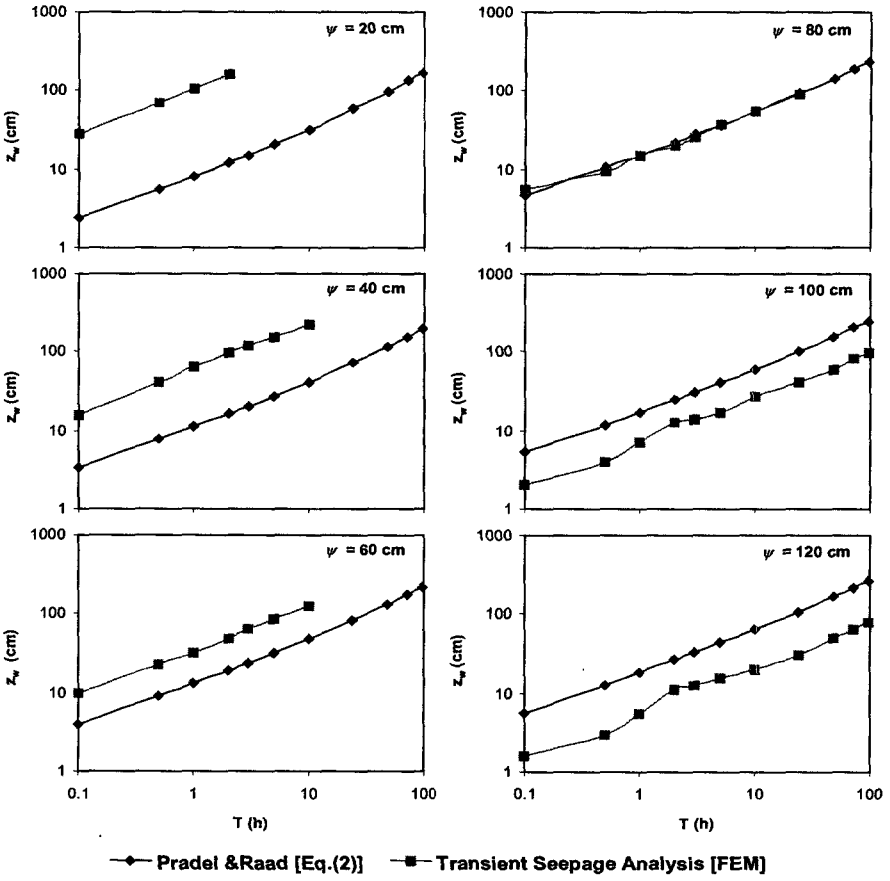

Fig. 7. Variation of Wetting Band Depth with Rainfall Duration - SW Soil

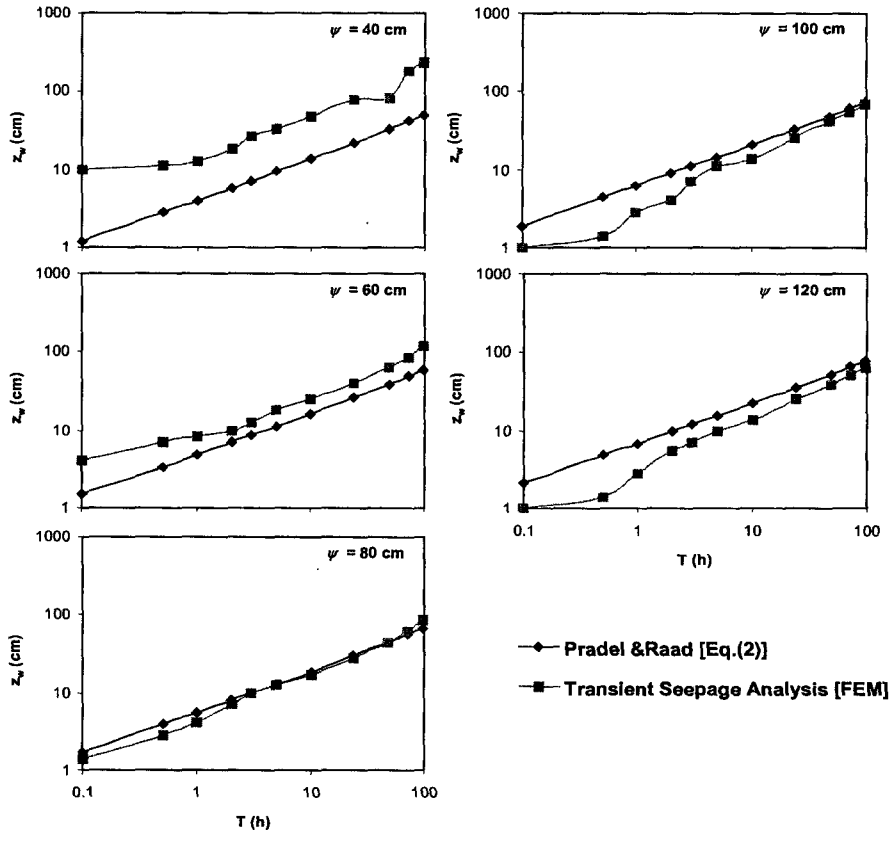

Fig. 8. Variation of Wetting Band Depth with Rainfall Duration - SM Soil

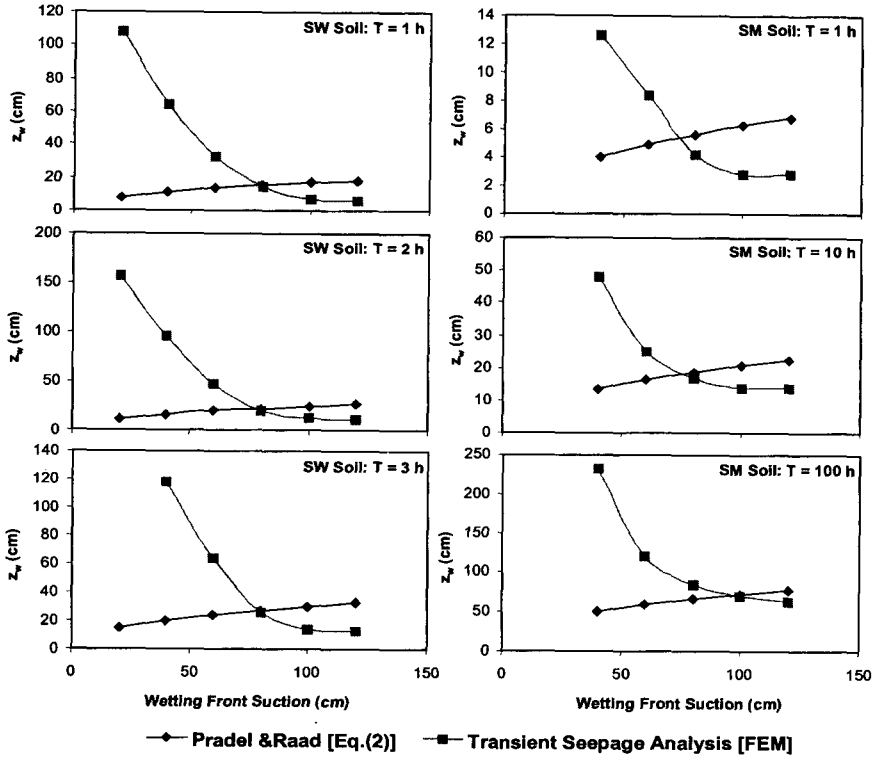

Fig. 9. Variation of Wetting Band Depth with Wetting Front Suction - SW and SM Soils

Eq. (2) and those obtained from numerical analysis can be attributed to the fact that Eq. (2) does not correlate z_w with the shear strength of the soil. On the other hand, for the results obtained from transient seepage analyses, critical z_w is considered a function of the shear strength of the soil. In other words, the failure plane needs not be located at the z_w value calculated using Eq. (2) for a given value of Ψ ; a shallower failure mechanism is possible if Ψ is greater than 80 cm.

7. Slope Stability Analysis

In order to assess the effect of wetting band depth and the magnitude of wetting front suction on the stability of slopes in weathered soils, two sets of analyses were conducted using the limit equilibrium based program SLOPE/W (Geo-Slope, 1998). For both sets, two infinite slopes - inclined at 27° and 45° with respect to horizontal - were considered. Fig. 10 defines the key parameters for the slope stability analyses. Table 3 gives the physical properties and shear strength parameters used in the slope stability analyses. It should be noted no testing was undertaken in the present study to establish the values given in Table 3. These are average values for typical weathered soils in Korea and are often used in Korean geotechnical practice. Therefore, no distinction will be

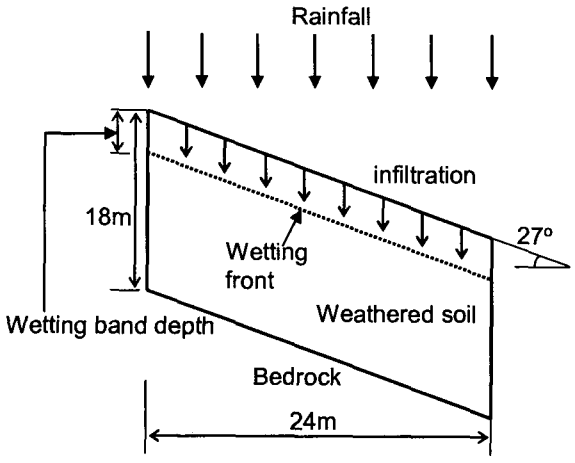

Fig. 10. Definition of Various Parameters for Slope Stability Analyses

Table 3. Strength Parameters for typical Korean Weathered Soils

Type	ρ (g/cm^3)	c' (kPa)	ϕ' (°)
Loose	1.7	10	25
Medium	1.8	10	29
Dense	1.9	10	33

made between SW and SM weathered soils when presenting the results of these slope stability analyses.

8. Effect of Wetting Band Depth on the Stability of Slope

In the first set of analyses, the effect of wetting band depth was investigated. Here, the wetting band depth was varied from 15 cm to 300 cm by specifying 100% degree of saturation within the wetting band. For the rest of the slope, the degree of saturation was estimated using initial volumetric water content values as shown in Table 2. The corresponding values of matric suction are estimated from the SWCC of the two weathered soils. SLOPE/W calculates the available shear strength of an unsaturated soil using matric suction, angle of internal friction ϕ' and an angle ϕ^b - slope of the Mohr-Coulomb failure envelope in the shear stress vs. matric suction space (Fredlund and Rahardjo, 1993), represented by Eq. (8) below:

$$\tau_f = c' + (\sigma_f - u_a)\tan\phi' + (u_a - u_w)\tan\phi^b \qquad (8)$$

where c' is the true cohesion due to cementation of soil particles, σ_f is the total normal stress at failure, u_a is the pore air pressure and u_w is the pore water pressure. The third term on the right-hand side of Eq. (8) represents apparent cohesion that is a function of soil matric suction (u_a - u_w). Vanapalli et al. (1996) have proposed the following relationship between ϕ^b, degree of saturation S and angle of internal friction ϕ':

$$\tan(\phi^b) = \tan(\phi')\left(\frac{S - S_r}{100 - S_r}\right) \qquad (9)$$

where S_r is the residual degree of saturation in percent. The values of ϕ^b given in Table 2 have been obtained using Eq. (9). As stated above, the main effect of ϕ^b is to induce apparent cohesion in the soil if the soil has some matric suction. The higher the matric suction, the higher is the value of apparent cohesion and consequently, the higher is the available shear strength.

The results of the first set of slope stability analyses are presented in Fig. 11. As expected, the factor of safety at zero wetting band depth was higher for 27° slope as compared to 45° slope. For both the slope angles, the factor of safety decreased gradually as the wetting band depth increased. When the wetting band depth was increased beyond 120 cm, there was a sharp decrease in factor of safety. Beyond a wetting band depth of 200 cm, the factor of safety changed insignificantly with wetting band depth. The critical depth of 120 cm is mainly influenced by the specified value of true cohesion c'. For soils with c' greater than 10 kPa, the critical depth would be greater than 120 cm. At z_w values greater than the critical depth, the stability of the slope is ensured mainly by the specified c'. For all these slope stability analyses, the failure mechanism was surficial and was contained within the wetting band.

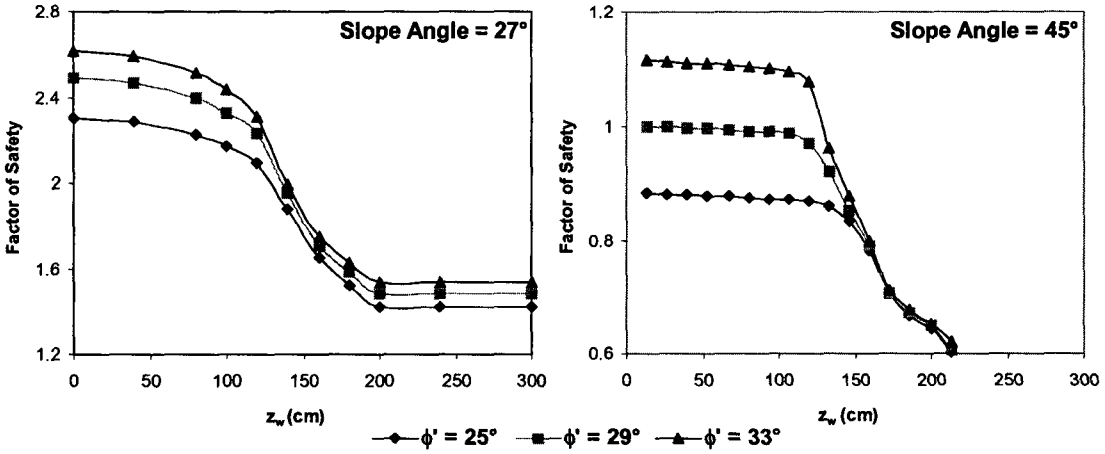

Fig. 11. Effect of Wetting Band Depth on Factor of Safety

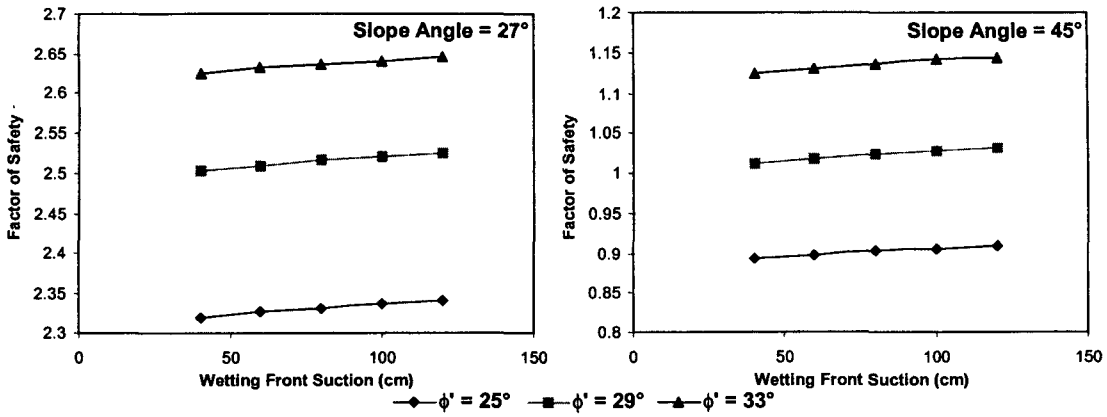

Fig. 12. Effect of Wetting Front Suction on Factor of Safety

9. Effect of Wetting Front Suction on Stability of Slopes

The second set of slope stability analyses investigated the effect of the magnitude of wetting front suction Ψ on the stability of slope. Here, the pressure heads calculated using a transient seepage analysis of rainfall infiltration using SEEP/W were used in SLOPE/W to establish the available shear strength of the soil. Several analyses were conducted at different Ψ values. Fig. 12 shows the results of the second set of slope stability analyses. It can be seen from Fig. 12 that an increase in Ψ results in a marginal increase in the factor of safety for the slope because of a higher apparent cohesion at higher wetting front suction values. It can also be seen that the contribution of c' and ϕ' outweighs the contribution of ϕ^b towards the stability of the slope.

10. Conclusions

A study of rainfall-induced instability in infinite slopes of typical Korean weathered soils (classified as SW and SM according to USCS) was undertaken using Pradel and Raad's (1993) modification of theoretical equations for the Green and Ampt (1911) model. The objective of this study was to establish the applicability of these theoretical equations to Korean weathered soils. The wetting band depth calculated using theoretical equations was compared with those obtained from finite element transient seepage and slope stability analyses. It was found that at wetting front suctions of less than 80 cm, the theoretical equations predicted lower wetting band depths than those predicted by the numerical analyses. At wetting front suctions greater than 80 cm, the theoretical equations predicted higher wetting band depths than those predicted by the numerical analyses. This finding is significant from the point-of-view of using the theoretical equations proposed by Pradel and Raad (1993) for Korean weathered soils that typically have wetting front suction values less than 40 cm (< 4 kPa). For such soils, these theoretical equations should be used with caution. The factor of safety of an infinite slope located in these weathered soils is found to reduce drastically when the wetting band depth is increased beyond 120 cm. This critical wetting band depth is closely linked to the value of true cohesion c' that is around 10 kPa for Korean weathered soils. There is also a marginal increase in the factor of safety when the wetting front suction is increased from 40 cm to 120 cm. Although such an increase in factor of safety is small, it can make a difference between stability and failure for slopes with factors of safety only slightly greater than unity. It should also be noted that the present study was focused on investigating the effect of infiltration of rainfall. Other effects such as evaporation and run-off were not considered. Both evaporation and run-off can reduce the amount of infiltration significantly. Therefore, the findings of the present study can be regarded as erring on the safe side.

References

1. ASTM (2000), *Annual Book of ASTM Standards: Measurement of Soil Potential (Suction) Using Filter Paper*. Vol.04.08, D5298-94, pp.154-159.
2. Chow, V. T., Maidment, D. R. and Mays, L. W. (1988), *Applied Hydrology*, McGraw-Hill, New York.
3. Fourie, A. B., Rowe, D. and Blight, G. E. (1999), "The effect of infiltration on the stability of the slopes of a dry ash dump", *Gé otechnique*, Vol.49, No.1, pp.1-13.
4. Fredlund, D. G. and Xing, A. (1994), "Equations for the soil-water characteristic curve", *Canadian Geotechnical Journal*, Vol.31, pp.521-532.
5. Fredlund, D. G. and Rahardjo, H. (1993), *Soil Mechanics for Unsaturated Soils*, John Wiley and Sons.
6. Geo-Slope (1998), *User's manual for SEEP/W and SLOPE/W: Version 4*, Geo-Slope International Ltd, Canada.
7. Green, W. H. and Ampt, G. A. (1911), "Studies on soil physics. 1: The flow of air and water through soils", *J. Agric. Sci.*, Vol.4, No.1, pp.1-24.
8. Holtz, R.D. and Kovacs, W.D. (1981), *An Introduction to Geotechnical Engineering*, Prentice-Hall Inc, USA.
9. Kim, S. I., Park, C. H., Lee, S. R. and Jeong, S. S. (1994), *Report of the Stability Analysis of Natural Slope of Yongseong Industrial Complex in Yeocheon*, Lucky-Development Company, Korea.
10. Lee, S. G. and de Freitas. M. H. (1989), "A revision of the description and classification of weathered granite and its application to granites in Korea", *J. of Engrg. Geol.*, Vol.22, No.1, pp.31-48.
11. Leong, E. C. and Rahardjo, H. (1997), "Review of Soil-Water Characteristic Curve Equations", *Journal of Geotechnical and Geoenvironmental Engineering*, Vol.123, No.12, pp.1106-1117.
12. Leong, E.C., He, L. and Rahardjo, H. (2002), "Factors affecting the filter paper method for total and matric suction measurements", *Geotechnical Testing Journal*, Vol.25, No.3, pp.1-12.
13. Lumb, P. B. (1962), "Effects of rain storms on slope stability", *Symp. on Hong Kong Soils*, Hong Kong, pp.73-87.
14. Lumb, P. B. (1975), "Slope failures in Hong Kong", *Q. J. Engng Geol*, Vol.8, pp.31-65.
15. Maidment, David R. (1993), *Handbook of hydrology. David R. Maidment*, McGraw-Hill, pp.5.32-5.51.
16. Moore, R. E. (1939), "Water conduction from shallow water tables", *Hilgardia*, Vol.12, No.6, pp.383-426.
17. Ng, C. W. W. and Shi, Q. (1998), "A numerical investigation of the stability of unsaturated soil slopes subjected to transient seepage", *Computers and Geotechnics*, Vol.22, No.1, pp.1-28.
18. Pradel D. and Raad G. (1993), "Effect of Permeability on Surficial Stability of Homogeneous Slopes", *Journal of Geotechnical Engineering*, Vol.119, No.2, pp.315-332.
19. Rahardjo, H., Lim, T. T., Chang, M. F., and Fredlund, D. G. (1995), "Shear-strength characteristics of a residual soil", *Canadian Geotechnical Journal*, Vol.32, pp.60-77.
20. Rawls, W. J., Brakensiek, D. L. and Soni, B. (1983), "Agricultural Management Effects on Soil Water Processes: Part I . Soil Water Retention and Green-Ampt Parameters. Trans", *American Society of Agricultural Engineers*, Vol.26, No,6, pp.1747-1752.
21. Skagg, R. W. and Khaleel, R. (1982), "Hydrologic Modeling of Small Watersheds, Monograph 5", *Infiltration.* In C.T. Haan, ed. American Society of Agricultural Engineers, St. Joseph, Mich., pp.4-166.
22. Van Genuchten, M. T. (1980), "A closed-form equation for predicting the hydraulic conductivity of unsaturated soils", *J. Soil Sci. Soc. Am.*, Vol.44, pp.892-898.
23. Vanapalli, S. K., Fredlund, K. G., Pufahl, D. E. and Clifton, A. W. (1996), "Model for prediction of shear strength with respect to matric suction", *Canadian Geotechnical Journal*, Vol.33, pp. 379-392.

(received on Aug. 17, 2004, accepted on Sep. 23, 2004)